Ultrahigh-energy neutrino scattering

Masaaki Kuroda*

Institute of Physics, Meiji Gakuin University, Kamikurata-cho 1518, Totsuka-ku, Yokohama 244-8539, Japan

Dieter Schildknecht†

Fakultät für Physik, Universität Bielefeld, D-33501 Bielefeld, Germany and Max-Planck Institute für Physik (Werner-Heisenberg-Institut), Föhringer Ring 6, D-80805 München, Germany

(Received 13 May 2013; published 17 September 2013)

We predict the neutrino-nucleon cross section at ultrahigh energies relevant in connection with the search for high-energy cosmic neutrinos. Our investigation, employing the color-dipole picture, among other things, allows us to quantitatively determine which fraction of the ultrahigh-energy neutrino-nucleon cross section stems from the saturation vs the color-transparency region. We disagree with various results in the literature that predict a strong suppression of the neutrino-nucleon cross section at neutrino energies above $E \cong 10^9$ GeV. Suppression in the sense of a diminished increase of the neutrino-nucleon cross section with energy only starts to occur at neutrino energies beyond $E \cong 10^{14}$ GeV.

DOI: 10.1103/PhysRevD.88.053007 PACS numbers: 13.15.+g, 13.60.Hb

Initiated by the experimental search for cosmic neutrinos of energies larger than $E \simeq 10^6$ GeV,[1] the theoretical investigation[2] of the neutrino-nucleon interaction at ultrahigh energies received much attention recently. Predictions require a considerable extension of the theory of neutrino-nucleon deep inelastic scattering (DIS) into a kinematic domain beyond the one where results from experimental tests are available at present. Different theoretical approaches have been employed, ranging from conventional linear evolution of nucleon parton distributions to the investigation of possible nonlinear effects conjectured to becoming relevant in the ultrahigh-energy domain.

In the present paper, we consider neutrino scattering in the framework of the color dipole picture (CDP).[3] The CDP is uniquely suited for a treatment of ultrahigh-energy neutrino scattering. Extrapolating the results from electron-proton scattering at HERA, we expect the total neutrino-nucleon cross section at ultrahigh energies to be dominantly due to the kinematic range of $x \ll 0.1$ of the Bjorken variable $x_{\mathrm{bj}} \equiv x \cong Q^2/W^2$. This is the domain of validity of the CDP.

In particular, we shall focus on the question of color transparency vs saturation. Does the total neutrino-nucleon cross section at ultrahigh energies dominantly originate from the region of large values of the low-x scaling variable [4,5],

$$\eta(W^2, Q^2) = \frac{(Q^2 + m_0^2)}{\Lambda^2_{\mathrm{sat}}(W^2)}, \tag{1}$$

namely, $\eta(W^2, Q^2) \gg 1$ (“color transparency” region), or is there a substantial part that is due to the kinematic range of $\eta(W^2, Q^2) \ll 1$ (“saturation” region)?

In Eq. (1), $\Lambda^2_{\mathrm{sat}}(W^2)$ denotes the “saturation scale” that increases with the $\gamma^*(Z^0, W^\pm)p$ center-of-mass energy squared, W^2, as $(W^2)^{C_2}$, where $C_2 \simeq 0.29$ [compare Eq. (12) below]. At HERA energies, $\Lambda^2_{\mathrm{sat}}(W^2)$ approximately ranges from $2\ \mathrm{GeV}^2 \lesssim \Lambda^2_{\mathrm{sat}}(W^2) \lesssim 7\ \mathrm{GeV}^2$. The $\gamma^*(Z^0, W^\pm)$ virtual four-momentum squared in Eq. (1) is denoted by $q^2 = -Q^2$, and $m_0^2 \simeq 0.15\ \mathrm{GeV}^2$ (for light quarks). Compare Fig. 1 for the (Q^2, W^2) plane with the line of $\eta(W^2, Q^2) = 1$.

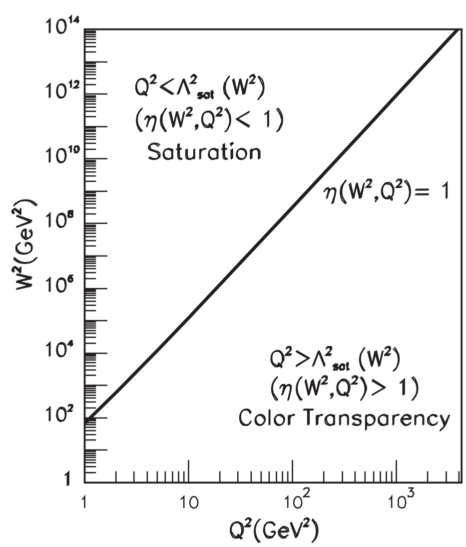

FIG. 1. The (Q^2, W^2) plane showing the line $\eta(W^2, Q^2) = 1$ that separates the saturation region from the color-transparency region.

*kurodam@law.meijigakuin.ac.jp
†schild@physik.uni-bielefeld.de
[1]Compare Refs. [16–24] in Ref. [1].
[2]Compare, e.g., Refs. [2–8] in Ref. [2].
[3]Compare Ref. [3] for recent reviews on the CDP and an extensive list of references.

The charged-current neutrino-nucleon cross section we shall concentrate on, as a function of the neutrino energy, E, is given by (e.g., Ref. [6])

$$\sigma_{\nu N}(E) = \int_{Q^2_{\min}}^{s-M_p^2} dQ^2 \int_{\frac{Q^2}{s-M_p^2}}^{1} dx \frac{1}{xs}\frac{\partial^2\sigma}{\partial x \partial y}, \tag{2}$$

where

$$\frac{\partial^2\sigma}{\partial x\partial y} = G_F^2 \frac{s}{2\pi}\left(\frac{M_W^2}{Q^2+M_W^2}\right)^2 \sigma_r(x, Q^2), \tag{3}$$

and $\sigma_r(x, Q^2)$ in Eq. (3) denotes the "reduced cross section"

$$\sigma_r(x, Q^2) = \frac{1+(1-y)^2}{2} F_2^\nu(x, Q^2) - \frac{y^2}{2} F_L^\nu(x, Q^2) + y\left(1-\frac{y}{2}\right) x F_3^\nu(x, Q^2). \tag{4}$$

In standard notation, s denotes the neutrino-nucleon center-of-mass energy squared,

$$s = 2M_p E + M_p^2 \cong 2M_p E, \tag{5}$$

with M_p being the nucleon mass, $q^2 = -Q^2$ is the four-momentum squared transferred from the neutrino to the $W^\pm$ boson of mass M_W, and G_F is the Fermi coupling. The Bjorken variable is given by

$$x = \frac{Q^2}{2qP} = \frac{Q^2}{W^2+Q^2-M_p^2} \cong \frac{Q^2}{W^2}, \tag{6}$$

where the approximate equality in Eq. (6) is valid in the relevant range of $x \ll 0.1$. The fraction of the energy transfer from the neutrino to the $W^\pm$ boson, y, is given by

$$y = \frac{Q^2}{2M_p E x} \cong \frac{W^2}{s}. \tag{7}$$

For the subsequent discussion, it will be useful to replace the integration over dx in Eq. (2) by an integration over W^2, rewriting Eq. (2) as

$$\sigma_{\nu N}(E) = \frac{G_F^2}{2\pi}\int_{Q^2_{\min}}^{s-M_p^2} dQ^2 \left(\frac{M_W^2}{Q^2+M_W^2}\right)^2 \times \int_{M_p^2}^{s-Q^2} \frac{dW^2}{W^2+Q^2-M_p^2}\sigma_r(x, Q^2). \tag{8}$$

Because of the vector-boson propagator, contributions to the total cross section for $Q^2 \gg M_W^2$ are strongly suppressed, and with $W^2 \le s$ and s in the ultrahigh-energy range, $s \gg M_W^2$, we expect the cross section to dominantly originate from $x \approx Q^2/W^2 \ll 0.1$.

In what follows, we concentrate on the (dominant) contribution due to $F_2^\nu(x, Q^2)$ in Eq. (8) according to Eq. (4).[4]

[4]The contribution due to $F_L^\nu(x, Q^2)$ turned out to be less than 6%; compare the discussion in connection with Table IV below. The contribution from the structure function $F_3(x, Q^2)$ in Eq. (4), that is due to valence-quark interactions, can be ignored.

For small values of $x \lesssim 0.1$, DIS of electrons and neutrinos on nucleons, in terms of, respectively, the imaginary part of the $\gamma^* p$ and the $(W^\pm, Z^0)p$ forward scattering amplitude, proceeds via scattering of long-lived massive hadronic fluctuations, $\gamma^*(Z^0) \to q\bar{q}$ and $W^- \to \bar{u}d$, etc., that undergo diffractive forward scattering on the nucleon (CDP) [3].

For the flavor-symmetric $(q\bar{q})N$ interaction at $x \ll 0.1$, the neutrino-nucleon structure function, $F_2^{\nu N}(x, Q^2)$, and the electromagnetic structure function, $F_2^{eN}(x, Q^2)$, are related by $(1/n_f)F_2^{\nu N}(x, Q^2) = (1/\sum_q Q_q^2)F_2^{eN}(x, Q^2)$, or

$$F_{2,L}^{\nu N}(x, Q^2) = \frac{n_f}{\sum_q^{n_f} Q_q^2} F_{2,L}^{eN}(x, Q^2), \tag{9}$$

where n_f denotes the number of actively contributing quark flavors, Q_q is the quark charge, and $n_f/\sum_q Q_q^2 = 18/5$ for $n_f = 4$ flavors of quarks. As a consequence of the proportionality (9), the total neutrino-nucleon cross section (8) may be predicted by inserting the electromagnetic structure function into Eq. (4).

The electromagnetic structure function, $F_2^{ep}(x, Q^2)$, is related to the total photoabsorption cross section, $\sigma_{\gamma^* p}(W^2, Q^2)$, by[5]

$$F_2^{ep}(x, Q^2) = \frac{Q^2}{4\pi^2\alpha}\sigma_{\gamma^* p}(W^2, Q^2). \tag{10}$$

In the CDP, as a consequence [4,5,7] of the interaction of the color dipole with the gluon field in the nucleon, the photoabsorption cross section becomes a function of the low-x scaling variable, $\eta(W^2, Q^2)$,

$$\sigma_{\gamma^* p}(W^2, Q^2) = \sigma_{\gamma^* p}(\eta(W^2, Q^2)) \sim \sigma^{(\infty)} \begin{cases} \ln\frac{1}{\eta(W^2,Q^2)} & \text{for } \eta(W^2, Q^2) \ll 1, \\ \frac{1}{2\eta(W^2,Q^2)} & \text{for } \eta(W^2, Q^2) \gg 1, \end{cases} \tag{11}$$

where the cross section $\sigma^{(\infty)} \equiv \sigma^{(\infty)}(W^2)$ is of hadronic size, and, at most, it depends weakly on W^2. Both the dependence on the single variable $\eta(W^2, Q^2)$ (for $\sigma^{(\infty)} \cong$ const) in Eq. (11) and the specific functional form of this dependence are general consequences [4,7] of the color-gauge-invariant interaction of a $(q\bar{q})$ dipole with the color field in the nucleon. Any specific ansatz for a parametrization of the dipole-nucleon cross section has to provide an interpolation between the $\ln(1/\eta(W^2, Q^2))$ and the $1/2\eta(W^2, Q^2)$ dependence in Eq. (11). It is well known [4], compare Fig. 2, that the dependence (11) on the single variable $\eta(W^2, Q^2)$ is fulfilled by the experimental data with $\sigma^{(\infty)} \cong$ const in the HERA energy range. The saturation scale is given by [4,5,7]

[5]The low-x approximation is used for the factor in front of $\sigma_{\gamma^* p}(W^2, Q^2)$ in Eq. (10).

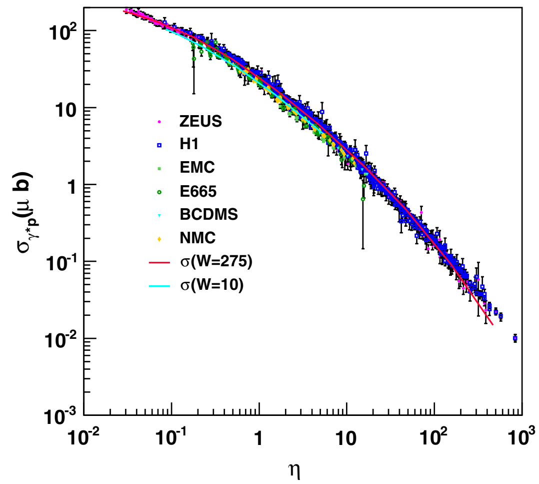

FIG. 2 (color online). The theoretical prediction [4,7] for the photoabsorption cross section $\sigma_{\gamma^* p}(\eta(W^2, Q^2))$ compared with the experimental data on DIS.

$$\Lambda^2_{\rm sat}(W^2) = C_1\left(\frac{W^2}{1\ {\rm GeV}^2}\right)^{C_2}, \qquad C_1 = 0.34\ {\rm GeV}^2, \qquad C_2 \cong 0.29. \tag{12}$$

The value of the exponent $C_2 \cong 0.29$ is fixed [7] by requiring consistency of the CDP with the perturbative-QCD-improved parton model.

We return to neutrino scattering. Employing relation (9), we replace the neutrino structure function, $F_2^\nu(x, Q^2)$, in Eq. (4) by the electromagnetic one, $F_2^{ep}(x, Q^2)$, or rather by the photoabsorption cross section; compare Eq. (10). The neutrino-nucleon total cross section (8) becomes[6]

$$\sigma_{\nu N}(E) = \frac{G_F^2 M_W^4}{8\pi^3\alpha}\frac{n_f}{\sum_q Q_q^2}\int_{Q^2_{\rm min}}^{s-M_p^2} dQ^2 \frac{Q^2}{(Q^2+M_W^2)^2} \times \int_{M_p^2}^{s-Q^2}\frac{dW^2}{W^2}\frac{1}{2}(1+(1-y)^2)\sigma_{\gamma^* p}(\eta(W^2, Q^2)). \tag{13}$$

We first of all look at the ratio

$$r(E) = \frac{\sigma_{\nu N}(E)_{\eta(W^2,Q^2)<1}}{\sigma_{\nu N}(E)}. \tag{14}$$

In Eq. (14), $\sigma_{\nu N}(E)_{\eta(W^2,Q^2)<1}$ denotes that part of the total neutrino-nucleon cross section in Eq. (13) that originates from contributions from the saturation region of $\eta(W^2, Q^2) < 1$ in Fig. 1. This part of the total cross section (13) is obtained by imposing the cut of $\eta(W^2, Q^2) < 1$ on the (Q^2, W^2) integration domain in Eq. (13). According to Eqs. (1) and (12), the restriction of $\eta(W^2, Q^2) < 1$ (for $Q^2_{\rm max} \geq Q^2 \geq Q^2_{\rm min} = \Lambda^2_{\rm sat}(M_p^2) - m_0^2$, and $Q^2_{\rm max} \gg m_0^2$) upon employing $W^2_{\rm max} = s - Q^2$ yields

$$W^2 \geq W^2(Q^2)_{\rm min} = \left(\frac{Q^2+m_0^2}{C_1}\right)^{\frac{1}{C_2}}, \qquad Q^2 \leq Q^2_{\rm max} = \Lambda^2_{\rm sat}(s)\left(1 - C_2\frac{\Lambda^2_{\rm sat}(s)}{s} + o\left(\frac{\Lambda^4_{\rm sat}(s)}{s^2}\right)\right). \tag{15}$$

From Eq. (15), for the ultrahigh energy corresponding to $s = 10^{14}$ GeV^2, with Eq. (12), one finds $Q^2 < Q^2_{\rm max} = \Lambda^2_{\rm sat}(s) = 3.9 \times 10^3$ GeV$^2 \ll s$. We observe that even for $s = 10^{14}$ GeV^2, the range of $Q^2 < Q^2_{\rm max}$ covered under restriction (15) is smaller than the $W^\pm$ mass squared, $M_W^2 \approx 6.4 \times 10^3$ GeV^2, that determines the maximum of the Q^2-dependent factor in Eq. (13). We accordingly expect a small value of $r(E) \ll 1$.

The ratio $r(E)$ in Eq. (14) is evaluated in two steps. In a first step, we only rely on the very general low-x scaling restrictions for $\sigma_{\gamma^* p}(\eta(W^2, Q^2))$ in Eqs. (11) with (12) and derive an upper bound on $r(E) < \bar{r}(E)$ on $r(E)$. In a second step, we introduce a concrete representation for $\sigma_{\gamma^* p}(\eta(W^2, Q^2))$ in the CDP that smoothly interpolates the regions of $\eta(W^2, Q^2) < 1$ and $\eta(W^2, Q^2) > 1$ in Eq. (11).

The ratio $r(E)$ in Eq. (14), upon substituting Eq. (13) and taking into account Eq. (15), becomes

$$r(E) = \frac{\int_{Q^2_{\rm min}}^{Q^2_{\rm max}(s)} dQ^2 \frac{Q^2}{(Q^2+M_W^2)^2}\int_{W^2(Q^2)_{\rm min}}^{s-Q^2}\frac{dW^2}{W^2}(1+(1-y)^2)\sigma_{\gamma^* p}(\eta(W^2,Q^2))}{\int_{Q^2_{\rm min}}^{s-M_p^2} dQ^2 \frac{Q^2}{(Q^2+M_W^2)^2}\int_{M_p^2}^{s-Q^2}\frac{dW^2}{W^2}(1+(1-y)^2)\sigma_{\gamma^* p}(\eta(W^2,Q^2))}. \tag{16}$$

Using the scaling behavior (11) for $\eta(W^2, Q^2) < 1$ and $\eta(W^2, Q^2) > 1$, we derive an upper limit,

$$r(E) < \bar{r}(E), \tag{17}$$

on the ratio $r(E)$ in Eq. (16). Appropriately substituting the behavior (11) of $\sigma_{\gamma^* p}(\eta(W^2, Q^2))$ into Eq. (16), and simplifying by putting $y = 0$ in the numerator and $y = 1$ in the denominator, an upper bound on $r(E)$ reads[7]

[6] We restrict ourselves to the dominant term $F_2^\nu(x, Q^2)$ in Eq. (4), ignoring $F_L(x, Q^2)$ and $F_3(x, Q^2)$.

[7] In the denominator of Eq. (18), we inserted the $1/2\eta(W^2, Q^2)$ dependence only valid for $\eta(W^2, Q^2) > 1$. We explicitly checked that the enlargement of the cross section as a consequence of this approximation amounts to only a few percent in the energy range up to $E \sim 10^{14}$ GeV under consideration.

$$\bar{r}(E) = \frac{2\int_{Q^2_{\min}}^{Q^2_{\max}(s)} dQ^2 \frac{Q^2}{(Q^2+M_W^2)^2} \int_{W^2(Q^2)_{\min}}^{s-Q^2} \frac{dW^2}{W^2} \ln\frac{1}{\eta(W^2,Q^2)}}{\int_{Q^2_{\min}}^{s-M_p^2} dQ^2 \frac{Q^2}{(Q^2+M_W^2)^2} \int_{M_p^2}^{s-Q^2} \frac{dW^2}{W^2} \frac{1}{2\eta(W^2,Q^2)}}. \tag{18}$$

For $\Lambda^2_{\rm sat}(s) < M_W^2 \ll s$, one finds that the numerator in Eq. (18) is approximately given by

$$N(E) = \frac{1}{2}\frac{1}{2C_2}\left(\frac{\Lambda^2_{\rm sat}(s)}{M_W^2}\right)^2 + o\left(\left(\frac{\Lambda^2_{\rm sat}(s)}{M_W^2}\right)^3\right). \tag{19}$$

The denominator in Eq. (18) becomes

$$D(E) = \frac{1}{2C_2}\left(\frac{\Lambda^2_{\rm sat}(s)}{M_W^2}\right)\left(1 + o\left(\frac{M_W^2}{s}\log\frac{M_W^2}{s}\right)\right). \tag{20}$$

Inserting Eqs. (19) and (20) into Eq. (18), we find the upper bound on $r(E)$,

$$r(E) < \bar{r}(E) = \frac{1}{2}\frac{\Lambda^2_{\rm sat}(s)}{M_W^2}. \tag{21}$$

Numerical values of $\bar{r}(E)$, using Eq. (12), are given in Table I, together with the results for $r(E)$ resulting from an explicit expression for $\sigma_{\gamma^* p}(\eta(W^2, Q^2))$ from the CDP to be discussed below.

According to Eq. (21) and Table I, the fraction of the total neutrino-nucleon cross section arising from the saturation region is strongly suppressed. The saturation region contributes less than a few percent, except for extremely ultrahigh energies of order $E \simeq 10^{14}$ GeV.

TABLE I. The upper bound, $\bar{r}(E) > r(E)$, on the fraction of the total neutrino-nucleon cross section originating from the saturation region of $\eta(W^2, Q^2) < 1$. The results for $\bar{r}(E)$ in the second column are based on Eq. (21) with Eq. (12). The results for $r(E)|_{\rm Table\ 3}$ are based on evaluating Eq. (16) upon substitution of Eq. (22) with Eq. (25). The results for $r(E)|_{\rm Table\ 4}$ are based on evaluating Eq. (16) upon substitution of Eq. (29) with Eq. (25).

E(GeV)	$\bar{r}(E)$	$r(E)\vert_{\rm Table3}$	$r(E)\vert_{\rm Table4}$
10^6	1.74×10^{-3}	1.40×10^{-3}	4.58×10^{-3}
10^{10}	2.51×10^{-2}	1.63×10^{-2}	2.55×10^{-2}
10^{14}	3.63×10^{-1}	1.76×10^{-1}	1.96×10^{-1}

We turn to an evaluation of the neutrino-nucleon cross section based on an explicit form of $\sigma_{\gamma^* p}(\eta(W^2, Q^2))$ in the CDP.

The CDP leads to a remarkably simple form of the photoabsorption cross section that moreover can be represented by a closed expression[8] [4,7],

$$\begin{aligned}\sigma_{\gamma^* p}(W^2, Q^2) &= \sigma_{\gamma^* p}(\eta(W^2, Q^2)) + O\left(\frac{m_0^2}{\Lambda^2_{\rm sat}(W^2)}\right) \\ &= \frac{\alpha R_{e^+e^-}}{3\pi}\sigma^{(\infty)}(W^2) I_0(\eta(W^2, Q^2)) \\ &\quad + O\left(\frac{m_0^2}{\Lambda^2_{\rm sat}(W^2)}\right),\end{aligned} \tag{22}$$

where

$$I_0(\eta(W^2, Q^2)) = \frac{1}{\sqrt{1+4\eta(W^2,Q^2)}} \ln\frac{\sqrt{1+4\eta(W^2,Q^2)}+1}{\sqrt{1+4\eta(W^2,Q^2)}-1} \cong \begin{cases} \ln\frac{1}{\eta(W^2,Q^2)} + O(\eta\ln\eta), & \text{for } \eta(W^2,Q^2) \to \frac{m_0^2}{\Lambda^2_{\rm sat}(W^2)}, \\ \frac{1}{2\eta(W^2,Q^2)} + O\left(\frac{1}{\eta^2}\right), & \text{for } \eta(W^2,Q^2) \to \infty, \end{cases} \tag{23}$$

and

$$R_{e^+e^-} = 3\sum_q Q_q^2. \tag{24}$$

Comparing Eqs. (22) and (23) with Eq. (11), one notes that Eq. (22) smoothly interpolates the regions of $\eta(W^2, Q^2) \ll 1$ and $\eta(W^2, Q^2) \gg 1$ in Eq. (11).

The (weak) energy dependence of the dipole cross section $\sigma^{(\infty)}(W^2)$ in Eq. (22) is determined by consistency of $\sigma_{\gamma^* p}(W^2, Q^2)$ with Regge behavior [4,9] in the photoproduction limit of $\sigma_{\gamma p}(W^2) = \sigma_{\gamma^* p}(W^2, Q^2 = 0)$ and, alternatively, by consistency with the double-logarithmic fit to photoproduction by the Particle Data Group,

$$\sigma^{(\infty)}(W^2) = \frac{3\pi}{R_{e^+e^-}\alpha}\frac{1}{\ln\frac{\Lambda^2_{\rm sat}(W^2)}{m_0^2}} \begin{cases} \sigma^{\rm Regge}_{\gamma p}(W^2), \\ \sigma^{\rm PDG}_{\gamma p}(W^2). \end{cases} \tag{25}$$

The fits to photoproduction, compare Refs. [4,9,10] (in units of mb, with W^2 in GeV^2) are explicitly given by

$$\begin{aligned}\sigma^{(a)}_{\gamma p}(W^2) &= 0.0635(W^2)^{0.097} + 0.145(W^2)^{-0.5}, \\ \sigma^{(b)}_{\gamma p}(W^2) &= 0.0677(W^2)^{0.0808} + 0.129(W^2)^{-0.4525} \\ \sigma^{(c)}_{\gamma p}(W^2) &= 0.003056\left(33.71 + \frac{\pi}{M^2}\ln^2\frac{W^2}{(M_p+M)^2}\right) \\ &\quad + 0.0128\left(\frac{(M_p+M)^2}{W^2}\right)^{0.462},\end{aligned} \tag{26}$$

[8] We note that the closed form for the photoabsorption cross section in Eq. (22) with Eq. (23) contains the simplifying assumption of "helicity independence" leading to $F_L^{ep} = 0.33F_2^{ep}$ rather than $F_L^{ep} = 0.27F_2^{ep}$. This simplifying approximation is unimportant in the present context. Compare Refs. [7,8] for the refinement that implies the result $F_L^{ep} = 0.27F_2^{ep}$ that is consistent with the HERA experimental observations.

TABLE II. The prediction of the neutrino-nucleon cross section, $\sigma_{\nu N}^{(a,b,c)}[\mathrm{cm}^2]$, from the CDP as a function of the neutrino energy, E[GeV]. Compare the text for details.

E	1.0E + 04	1.0E + 06	1.0E + 08	1.0E + 10	1.0E + 12	1.0E + 14
$\sigma_{\nu N}^{(a)}$	1.28E − 34	1.91E − 33	1.09E − 32	5.36E − 32	2.60E − 31	1.23E − 30
$\sigma_{\nu N}^{(b)}$	1.21E − 34	1.68E − 33	8.96E − 33	4.11E − 32	1.85E − 31	8.15E − 31
$\sigma_{\nu N}^{(c)}$	1.19E − 34	1.69E − 33	9.26E − 33	4.29E − 32	1.88E − 31	7.77E − 31

where M_p stands for the proton mass and $M = 2.15$ GeV. Concerning the energy dependence of the photoabsorption cross section in Eq. (22), we note that the growth $\sigma_{\gamma^* p}(W^2, Q^2) \sim (\ln W^2)(W^2)^{C_2}$ in the color-transparency region (for $\sigma^{(\infty)}(W^2) \sim \sigma_{\gamma p}^{\mathrm{PDG}}(W^2)/\ln \frac{\Lambda_{\mathrm{sat}}^2(W^2)}{m_0^2}$) of $\eta(W^2, Q^2) > 1$ turns into the slower growth of $\sigma_{\gamma^* p}(W^2, Q^2) \sim (\ln W^2)^2$, once the saturation limit of $\eta(W^2, Q^2) < 1$ is reached.

In Table II, we present the results for the neutrino-nucleon cross section based on Eq. (13)[9] upon substitution of the photoabsorption cross section from Eq. (22) with $\Lambda_{\mathrm{sat}}^2(W^2)$ from Eq. (12), $m_0^2 = 0.15\ \mathrm{GeV}^2$ and $\sigma^{(\infty)}(W^2)$ determined by Eqs. (25) and (26). The results in Table II for $\sigma_{\nu N}^{(b)}(E)$ and $\sigma_{\nu N}^{(c)}(E)$ based on $\sigma^{(\infty)}(W^2)$ from the Regge fit (b) and the PDG fit (c), respectively, coincide in good approximation. The enhancement of the cross section $\sigma_{\nu N}^{(a)}(E)$ relative to $\sigma_{\nu N}^{(b,c)}(E)$ is a consequence of the stronger increase of the Pomeron contribution ($(W^2)^{0.097}$ vs $(W^2)^{0.0808}$) in $\sigma^{(\infty)}(W^2)$ originating from Eq. (26). At the highest energy under consideration, $E = 10^{14}$ GeV, the enhancement reaches a factor of about 1.5. Concerning the energy dependence, by comparing neighboring results in Table II for $E \geq 10^8$ GeV, one notes an increase (only) slightly stronger than expected from the proportionality to $\Lambda_{\mathrm{sat}}^2(s) \sim s^{C_2}$ in the estimate (20). This is a consequence of the energy dependence (25) of $\sigma^{(\infty)} = \sigma^{(\infty)}(W^2)$ ignored in Eq. (20).

We return to the question of the relative contribution to the neutrino cross section from the saturation region relative to the color-transparency region. We subdivide the neutrino cross section into the sum

$$\sigma_{\nu N}^{(c)}(E) = \sigma_{\nu N}^{(c)}(E)_{\eta(W^2,Q^2)<1} + \sigma_{\nu N}^{(c)}(E)_{\eta(W^2,Q^2)>1}. \quad (27)$$

The results are shown in Table III. From Table III, one finds that the fraction of the total cross section originating from the saturation region, $r(E)$ in Eqs. (14) and (16), increases from $r(E = 10^6\ \mathrm{GeV})|_{\mathrm{Table\ 3}} \cong 1.40 \cdot 10^{-3}$ to $r(E = 10^{14}\ \mathrm{GeV})|_{\mathrm{Table\ 3}} \cong 1.76 \cdot 10^{-1}$. The increase is consistent with the upper bound (21); compare Table I. With increasing energy, there is a strong increase of the contribution due to the saturation region, but even at $E = 10^{14}$ GeV the saturation region contributes only 17% approximately.

The result that the dominant part of the neutrino-nucleon cross section is due to contributions from large values of $\eta(W^2, Q^2) \gg 1$ requires further examination. For, e.g., a value of $Q^2 = 10^4\ \mathrm{GeV}^2 \cong M_W^2$, and for W^2 below $W^2 \leq 10^5\ \mathrm{GeV}^2$ (or $x \leq 0.1$), one finds that $\eta(W^2, Q^2)$ reaches values of $\eta(W^2, Q^2) \leq \eta_{\mathrm{Max}}(W^2, Q^2) \cong 10^3$. For such large values of $\eta(W^2, Q^2)$, as previously analyzed [4,7], the theoretical expression (22) for the photoabsorption cross section must be corrected by elimination of contributions from high-mass $(q\bar{q})$ fluctuations, $\gamma^* \to q\bar{q}$, of mass $M_{q\bar{q}}$. The lifetime of high-mass fluctuations in the rest frame of the nucleon becomes too short to be able to actively contribute to the $q\bar{q}$-color-dipole interaction. The restriction on the $q\bar{q}$ mass, $m_0^2 \leq M_{q\bar{q}}^2 \leq m_1^2(W^2)$, is taken care of by the energy-dependent upper bound, $m_1^2(W^2)$, where

$$m_1^2(W^2) = \xi \Lambda_{\mathrm{sat}}^2(W^2), \quad (28)$$

and empirically $\xi = 130$ [7]. Employing the restriction (28) extends the validity of the CDP to high values of $\eta(W^2, Q^2) \gg 1$.

Explicitly, one finds that Eq. (22) must be modified by a factor that depends on the ratio of $\xi/\eta(W^2, Q^2)$. One obtains [7]

$$\begin{aligned}\sigma_{\gamma^* p}(W^2, Q^2) &= \frac{\alpha R_{e^+e^-}}{3\pi} \sigma^{(\infty)}(W^2) I_0(\eta(W^2, Q^2)) \frac{1}{3}\left(G_L\left(\frac{\xi}{\eta(W^2, Q^2)}\right)\right. \\ &\quad \left. + 2G_T\left(\frac{\xi}{\eta(W^2, Q^2)}\right)\right) + O\left(\frac{m_0^2}{\Lambda_{\mathrm{sat}}^2(W^2)}\right), \end{aligned} \quad (29)$$

where

$$\begin{aligned}&\frac{1}{3}\left(G_L\left(\frac{\xi}{\eta(W^2, Q^2)}\right) + 2G_T\left(\frac{\xi}{\eta(W^2, Q^2)}\right)\right) \\ &= \frac{1}{\left(1 + \frac{\xi}{\eta(W^2,Q^2)}\right)^3}\left(\left(\frac{\xi}{\eta(W^2, Q^2)}\right)^3\right. \\ &\quad \left. + 2\left(\frac{\xi}{\eta(W^2, Q^2)}\right)^2 + \left(\frac{\xi}{\eta(W^2, Q^2)}\right)\right) \\ &\cong \begin{cases} 1 & \text{for } \eta(W^2, Q^2) \ll \xi = 130 \\ \frac{\xi}{\eta(W^2,Q^2)} & \text{for } \eta(W^2, Q^2) \gg \xi = 130 \end{cases}. \end{aligned} \quad (30)$$

[9] The CDP contains the limit of $Q^2 \to 0$, such that $Q_{\min}^2$ may be put to $Q_{\min}^2 = 0$ in Eq. (13). The actual dependence on $Q_{\min}^2$ is negligible, as long as $0 \lesssim Q_{\min}^2 \lesssim M_p^2$. We also note that the replacement of the lower limit $W^2 \geq M_p^2$ by $W^2 \geq \mathrm{const}\, M_p^2$ for, e.g., const ≤ 20 leads to an insignificant change of the neutrino cross section.

TABLE III. The contributions to the neutrino-nucleon cross section $\sigma^{(c)}_{\nu N}(E)[\mathrm{cm}^2]$ as a function of E[GeV] from the color transparency ($\eta(W^2, Q^2) > 1$) and the saturation ($\eta(W^2, Q^2) < 1$) region compared with the full cross section, $\sigma^{(c)}_{\nu N}(E)$, taken from Table II.

E	1.0E + 04	1.0E + 06	1.0E + 08	1.0E + 10	1.0E + 12	1.0E + 14
$\sigma^{(c)}_{\nu N}$	1.19E − 34	1.69E − 33	9.26E − 33	4.29E − 32	1.88E − 31	7.77E − 31
$\eta > 1$	1.19E − 34	1.68E − 33	9.22E − 33	4.22E − 32	1.77E − 31	6.41E − 31
$\eta < 1$	1.14E − 37	2.37E − 36	4.15E − 35	6.97E − 34	1.08E − 32	1.37E − 31

TABLE IV. The neutrino-nucleon cross section, $\sigma^{(c)}_{\nu N}(E)[\mathrm{cm}^2]$, as a function of the neutrino energy E[GeV] upon imposing the restriction (28) on the mass of actively contributing $q\bar{q}$ fluctuations (third and fourth lines) compared with the result from Table III (second line) that ignores the restriction (28). The results in the third and fourth lines are based on $\Lambda^2_{\mathrm{sat}}(W^2) \sim (W^2)^{C_2}$ with $C_2 = 0.29$ and $C_2 = 0.27$, respectively.

E	1.0E + 04	1.0E + 06	1.0E + 08	1.0E + 10	1.0E + 12	1.0E + 14
	1.19E − 34	1.69E − 33	9.26E − 33	4.29E − 32	1.88E − 31	7.77E − 31
$\sigma^{(c)}_{\nu N}$	3.85E − 35	5.15E − 34	4.17E − 33	2.73E − 32	1.49E − 31	6.96E − 31
	3.19E − 35	3.80E − 34	2.83E − 33	1.75E − 32	9.12E − 32	4.11E − 31

We note in passing that the theoretical prediction shown in Fig. 2 includes [7] the correction factor in (29) that, according to (30), becomes most relevant for values of $\eta(W^2, Q^2) \gtrsim 130$.

In Table IV, the third and fourth lines, we present our final results for the neutrino-nucleon cross section based on substituting Eq. (29)[10] into Eq. (13). The PDG result for $\sigma^{(\infty)}(W^2)$ in Eq. (25) is used, and, for comparison, the result for $\sigma^{(c)}_{\nu N}(E)$ from Table II [i.e., $\sigma^{(c)}_{\nu N}(E)$ without the restriction (28)] is again shown in the second line of Table IV. We explicitly verified that the addition in Eq. (13) of the contribution corresponding to the longitudinal structure function according to Eq. (4) diminishes the neutrino cross section in Table IV by less than 6% in the whole range of neutrino energies under consideration. To demonstrate the sensitivity under variation of the exponent C_2 of the energy dependence of the saturation scale, $\Lambda^2_{\mathrm{sat}}(W^2) \sim (W^2)^{C_2}$, in Table IV, we give the neutrino-nucleon cross section for $C_2 = 0.29$ and $C_2 = 0.27$. Both values are consistent with the available experimental information on DIS.

The results from Table IV (second and third lines) are graphically represented in Fig. 3. With increasing neutrino energy, the exclusion of inactive large-mass $q\bar{q}$ fluctuations by the restriction of $M^2_{q\bar{q}} < m^2_1(W^2) = \xi\Lambda^2_{\mathrm{sat}}(W^2)$, where $\xi = 130$, becomes less important. Most of the contributions to the neutrino-nucleon cross section in the extreme ultrahigh-energy limit ($E \simeq 10^{14}$ GeV) are due to moderately large values of $\eta(W^2, Q^2)$ that correspond to $q\bar{q}$ fluctuations of sufficiently long lifetime. Quantitatively, from Table IV, at $E = 10^4$ GeV the cross section is diminished by a factor of 0.32, while at $E = 10^{14}$ GeV this factor is equal to 0.89. This effect is also seen in the ratio $r(E)$ in Table I. At $E = 10^6$ GeV, the ratio $r(E)$ exceeds the crude estimate of $\bar{r}(E)$ from Eq. (18).

In Fig. 4, we compare our final results for the neutrino-nucleon cross section, $\sigma_{\nu N}(E) \equiv \sigma^{(c)}_{\nu N}(E)$ from Table IV, third and fourth line, based on the CDP, with the ones obtained [1,2] by employing the parton distributions from a conventional perturbative QCD (pQCD) analysis of DIS. Figure 4 shows consistency of our CDP results with the ones from the pQCD-improved parton model. Our predictions are also consistent with the ones in Ref. [11].

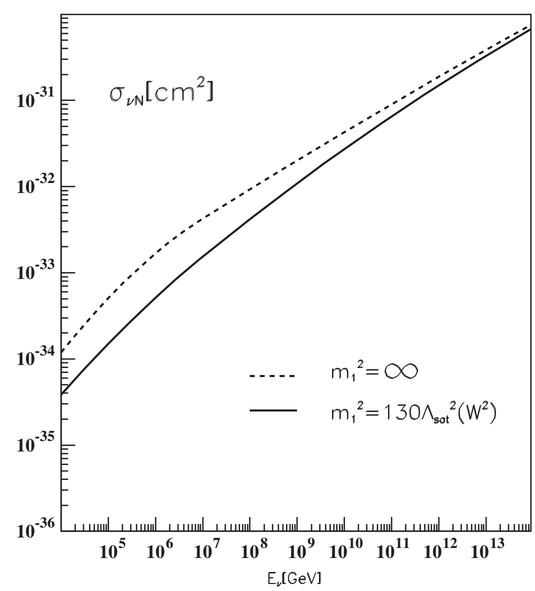

FIG. 3. The effect on the neutrino-nucleon cross section of excluding inactive high-mass $q\bar{q}$ fluctuations.

[10]We have verified that substitution of instead of Eq. (29), the photoabsorption cross section from Ref. [7] (compare footnote [8]) does not significantly affect the results for the neutrino-nucleon cross section.

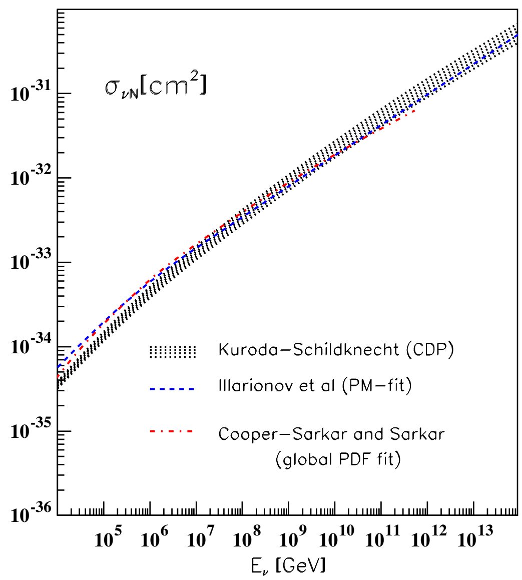

FIG. 4 (color online). Comparison of the CDP prediction for the neutrino-nucleon cross section, $\sigma_{\nu N}(E)[\mathrm{cm}^2]$, according to Eq. (13) with Eq. (29) and $\sigma_{\gamma p}^{\mathrm{PDG}}(W^2)$ from Eq. (25), with the predictions from the perturbative-QCD-improved parton model. The band of the prediction from the CDP illustrates the sensitivity of $\sigma_{\nu N}(E)$ under variation of the exponent C_2 in $\Lambda_{\mathrm{sat}}^2(W^2) \sim (W^2)^{C_2}$ between $C_2 = 0.27$ and $C_2 = 0.29$.

A series of recent papers [12–15] treats DIS at HERA energies and ultrahigh-energy neutrino scattering by adopting an ansatz with a $(\ln W^2)^2$ dependence of the underlying hadron-nucleon cross section. The ansatz is based on the asymptotic behavior of strong-interaction cross sections as $(\ln W^2)^2$ due to Heisenberg [16] and Froissart [17].

The ansatz of $F_2^{ep}(x, Q^2) \sim \sum_{n,m=0,1,2} a_{nm} (\ln Q^2)^n \times (\ln(1/x))^m$, with seven free fit parameters [12–15], yields a successful representation of the HERA experimental results for all x and Q^2 in the region of $x \lesssim 0.1$. The subsequent evaluation [12–15] of the neutrino-nucleon cross section with this ansatz for $F_2^{ep}(x, Q^2)$, essentially according to Eqs. (9) and (13), for $E \gtrsim 10^9$ GeV led to a cross section that is suppressed relative to pQCD results and is, consequently, also in comparison with our CDP predictions. Compare Fig. 5.

Since the CDP contains a $(\ln W^2)^2$ dependence, compare, e.g., the discussion immediately following Eq. (26), the result of Fig. 5 may look like an inconsistency. The apparent inconsistency is resolved in Fig. 6. Figure 6 shows the prediction for the neutrino-nucleon cross section from the CDP for an extended energy range up to $E = 10^{24}$ GeV. As seen in Fig. 6, in consistency with the $(\ln W^2)^2$ dependence of $\sigma_{\gamma^* p}(W^2, Q^2)$ in the saturation region of $\eta(W^2, Q^2) < 1$, also the CDP implies a decreasing growth of the neutrino-nucleon cross section. In distinction from the prediction from the Froissart-inspired ansatz, the decreasing growth of the cross section in the CDP is shifted to energies above $E \cong 10^{14}$ GeV.

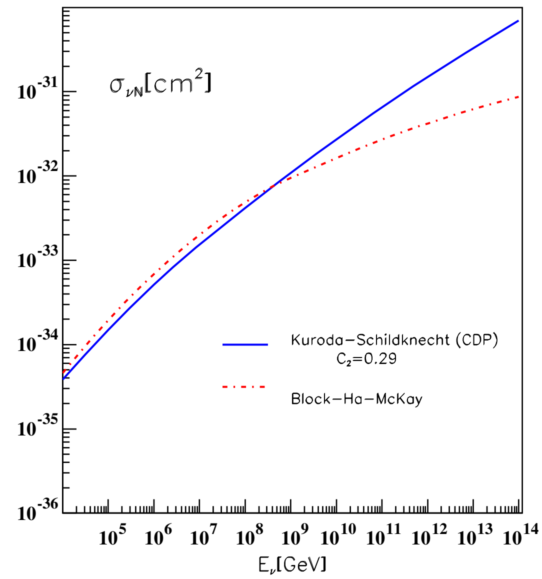

FIG. 5 (color online). A comparison of the results for the neutrino-nucleon cross section from the CDP according to Fig. 4 with the results from the "Froissart-inspired" ansatz from Ref. [14].

In Fig. 6, we explicitly demonstrate that the reduced growth of the neutrino cross section with increasing energy is directly connected with the increasingly smaller contribution due to $\sigma_{\nu N}^{(c)}(E)_{\eta(W^2,Q^2)>1}$ in Eq. (27). In the ultra-ultrahigh-energy limit, the neutrino-nucleon cross section

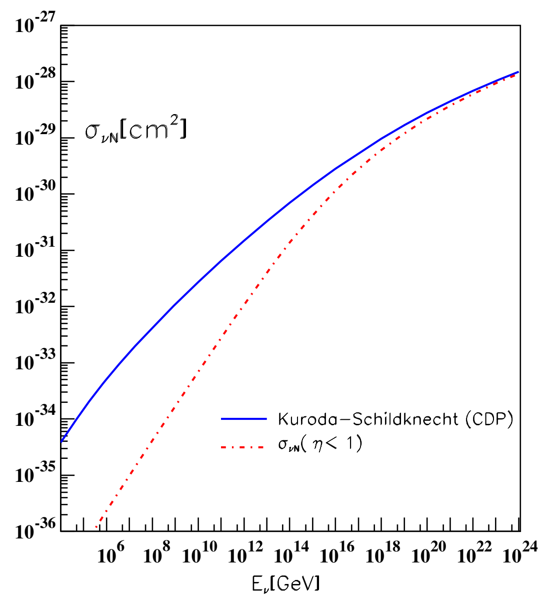

FIG. 6 (color online). The neutrino-nucleon total cross section, $\sigma_{\nu N}(E) \equiv \sigma_{\nu N}^{(c)}(E)$, from the CDP as a function of the neutrino energy E for the extended range of energies up to $E = 10^{24}$ GeV. For comparison, we also show that part of the cross section, $\sigma_{\nu N}(E)|_{\eta(W^2,Q^2)<1}$, that is obtained upon restricting the contributions of $\sigma_{\gamma^* p}(W^2, Q^2)$ to the neutrino-nucleon cross section to the saturation region of $\eta(W^2, Q^2) < 1$.

in Eq. (13) becomes saturated by contributions from that region of the photoabsorption cross section where the $(\ln(W^2))^2$ dependence becomes dominant.

We must conclude that the requirement of a "Froissart-like" ansatz for the underlying hadron-nucleon cross section *by itself does not* imply a weaker growth, compared with, e.g., the pQCD prediction, for the neutrino-nucleon cross section above $E = 10^9$ GeV. It is the combination of the energy dependence for $F_2^{ep}(x, Q^2)$, contained in $\ln(1/x)$ and $(\ln(1/x))^2$ terms, with the seven-free-parameter fit to the *ad hoc* polynomial $\ln Q^2$ dependence of the coefficients of the $\ln(1/x)$ and $(\ln(1/x))^2$ terms that leads to a suppression above $E = 10^9$ GeV.

In the CDP, the Q^2 dependence is uniquely fixed by the Q^2 dependence of the "photon-wave function," i.e., the transition of the (virtual) photon to $q\bar{q}$ dipole states with subsequent propagation of these $q\bar{q}$ states of mass $M_{q\bar{q}}$. The interaction of the $q\bar{q}$ color dipoles is restricted by being a gauge-invariant interaction with the gluon field in the nucleon.

Taking into account the more detailed dynamics of the CDP, and the much smaller number of free fit parameters, compared with the $\ln(1/x)$ and $(\ln(1/x))^2$ ansatz, we are thus led to disagree with the conclusion of an onset of a suppression of the neutrino-nucleon cross section for $E \gtrsim 10^9$ GeV implied by the analysis [12–15] of the Froissart-inspired ansatz.

A suppression, in the sense of a reduced growth of the total neutrino-nucleon cross section with increasing energy, is expected to occur, however, for neutrino energies beyond $E = 10^{14}$ GeV.

Questions on the subject matter by Paolo Castorina and by participants of the Oberwoelz symposium on Quantum Chromodynamics, History and Prospects (Oberwoelz, Austria, September 3–8, 2012) are gratefully acknowledged.

[1] A. Cooper-Sarkar and S. Sarkar, J. High Energy Phys. 01 (2008) 075.

[2] A. Yu. Illarionov, B. A. Kniehl, and A. V. Kotikov, Phys. Rev. Lett. **106**, 231802 (2011); M. M. Block, P. Ha, and D. W. McKay, arXiv:1110.6665v1.

[3] D. Schildknecht, Nucl. Phys. B, Proc. Suppl. **222–224**, 108 (2012); in 50th International School of Subnuclear Physics, Erice, Italy, 2012, arXiv:1210.0733v1 (to be published); AIP Conf. Proc. **1523**, 329 (2012).

[4] D. Schildknecht, Nucl. Phys. B, Proc. Suppl. **99**, 121 (2001); D. Schildknecht, B. Surrow, and M. Tentyukov, Phys. Lett. B **499**, 116 (2001); G. Cvetic, D. Schildknecht, B. Surrow, and M. Tentyukov, Eur. Phys. J. C **20**, 77 (2001).

[5] D. Schildknecht, in *DIS 2001, 9th International Workshop on Deep Inelastic Scattering, Bologna, Italy, 2001*, edited by G. Brassi *et al.* (World Scientific, Singapore, 2002), p. 798; D. Schildknecht, B. Surrow, and M. Tentyukov, Mod. Phys. Lett. A **16**, 1829 (2001).

[6] V. P. Gonçalves and P. Hepp, Phys. Rev. D **83**, 014014 (2011).

[7] M. Kuroda and D. Schildknecht, Phys. Rev. D **85**, 094001 (2012).

[8] M. Kuroda and D. Schildknecht, Phys. Lett. B **670**, 129 (2008); D. Schildknecht, Phys. Lett. B **716**, 413 (2012).

[9] S. Donnachie and P. Landshoff, Phys. Lett. B **296**, 227 (1992).

[10] J. Beringer *et al.* (Particle Data Group), Phys. Rev. D **86**, 010001 (2012).

[11] R. Fiore, L. L. Jenkovszky, A. V. Kotikov, F. Paccanoni, A. Papa, and E. Predazzi, Phys. Rev. D **68**, 093010 (2003); R. Fiore, L. L. Jenkovszky, A. V. Kotikov, F. Paccanoni, and A. Papa, Phys. Rev. D **73**, 053012 (2006).

[12] M. M. Block, E. Berger, and C.-I. Tan, Phys. Rev. Lett. **97**, 252003 (2006); E. Berger, M. Block, and C.-I. Tan, Phys. Rev. Lett. **98**, 242001 (2007).

[13] E. Berger, M. M. Block, D. McKay, and C.-I. Tan, Phys. Rev. D **77**, 053007 (2008).

[14] M. M. Block, P. Ha, and D. McKay, Phys. Rev. D **82**, 077302 (2010).

[15] M. M. Block, L. Durand, P. Ha, and D. W. McKay, arXiv:1302.6119v2; , arXiv:1302.6172v1.

[16] W. Heisenberg, in *Vorträge über Kosmische Strahlung*, (Springer, Berlin, 1953), p. 155; reprinted in W. Heisenberg, *Collected Works* (Springer, Berlin, 1984), Series B, p. 498; Die Naturwissenschaften **61**, 1 (1974); reprinted in W. Heisenberg, *Collected Works* (Springer, Berlin, 1984), Series B, p. 912.

[17] M. Froissart, Phys. Rev. **123**, 1053 (1961).